Scattering lens for Structured Illumination Microscopy

ARCHANA MALAVALLI AND CHRISTOF M. AEGERTER

Physik Institut, University of Zurich, Winterthurerstrasse 190, 8057 Zürich
aegerter@physik.uzh.ch

Abstract: In this article we describe a way to obtain beyond diffraction limited imaging capability behind a scattering medium using Structured Illumination Microscopy (SIM). A scattering medium such as a ground glass diffuser or a biological material poses obstacles to image formation, let alone high resolution imaging. However, building on the work of Vellekoop *et al.* [1] that transforms a scattering medium into a lens, we have previously demonstrated a technique to generate an array of focal spots behind a scattering medium [2]. Using such focal spot arrays, we illuminate fluorescent beads hidden behind a scattering medium. We process the recorded fluorescence images using an SIM reconstruction algorithm to reveal images beyond the limit of resolution of the scattering lens.

1. Introduction

Flourescence Microscopy is a ubiquitous tool for bioimaging. The resolution of a microscope has long been considered limited by the diffraction of light, also called Abbe's diffraction limit [3]. However, the recent past has seen the emergence of various imaging modalities that break this diffraction barrier such as NSOM [4], STED [5], STORM/PALM [6] [7]. These techniques make use of special mechanisms to narrow the Point Spread Function (PSF) of the microscope, thereby enhancing the resolution. The narrowing of the PSF is achieved either by a specially tailored light source and/or by exploiting the non-linear nature of fluorescent dyes. The technique of linearly Structured Illumination Microscopy (SIM) on the other hand achieves a resolution enhancement up to a factor of two by employing spatially patterned illumination [8] and hence works for any light source or fluorescent dye.

Although efficient in improving the resolution of an imaging system, these methods are inherently designed to address imaging optically thin specimens and offer limited penetration depth through the specimens, typically to a few tens or hundreds of microns. Penetration depth is greatly affected due to scattering of light. Spectroscopic and tomographic approaches such as Diffuse wave spectroscopy & tomography [9] and OCT [10] attempt to image deep inside biological tissues by collecting unscattered photons, albeit at much lower resolution. So one clearly sees a trade-off between achievable resolution and penetration depth.

With the advent of wavefront shaping and interferometric focusing of light [11], the problem of microscopy can be seen in a very different perspective. Using wavefront shaping, light can be made to focus through thick multiply scattering materials [12]. Moreover the ability to control the scattered light makes it that light scattering is no more a hindrance to imaging. Therefore by utilising interferometric focusing and the translation invariance of the obtained focus due to memory effect [13], a scattering medium is transformed into a lens. Such a scattering lens can be used for imaging samples hidden behind the medium [1] [14] [12], with resolution similar to widefield fluorescence microscopes in the multiple scattering regime.

Interferometric focusing has made it possible to explore different ways to image through multiply scattering materials. Diffraction limited imaging behind scattering medium has been demonstrated by multiple different groups [15] [16] [17] [18]. However one also attempts to go beyond the diffraction limit to explore the possibilities of super resolution microscopy behind

scattering media. van Putten *et al.* [19] have previously shown that by folding multiple scattering paths through a scattering material, its NA(Numerical Aperture) can be increased greatly, thereby narrowing the corresponding PSF of the imaging system [20]. However the detection PSF would be still limited by diffraction. This leads to the fact that the sample response has to be extracted by computational means.

In order to reliably extract high resolution information from the sample illuminated with a scattering lens, we make use of Structured Illumination Microscopy(SIM) technique. The spatially periodic illumination required for SIM can be generated behind a multiply scattering material using our preciously demonstrated technique [2]. In this article we further apply such patterned illumination to image fluorescent structures hidden behind scattering media. We show that using SIM, we can reconstruct high resolution information from these images and thereby improving the resolution of the microscope beyond diffraction limit.

2.   Experimental Preliminaries

Figure 1 shows a part of the experimental setup used to generate multiple foci behind a scattering medium. The detailed experimental setup is provided in Malavalli *et al.* [2]. In our experiments, incoming light is spatially modulated using a spatial light modulator (SLM) before it passes through an illumination objective and hits the sample made up of a ground glass diffuser with a thickness of 1 mm. The diffuser randomizes the incoming light and forms a speckle pattern in the far field i.e on the detecting camera, however does not lead to an increased width of illumination and hence effective NA as would be the case for a thick turbid medium. The illumination lens system is optimised so as to obtain an average speckle size of the order of diffraction limit of the detection system. The smooth surface of the diffuser is coated with fluorescent beads to provide the fluorescence response required for imaging them.

The calibration of the microscope involves determining the experimental PSF of the system. For this purpose, images of isolated 0.5μm fluorescent beads were recorded by illuminating them in a wide-field mode. From these recorded images, the intensity profile of the fluorescence emission, which is typically a Gaussian distribution, was determined. The thus measured PSF and its corresponding Fourier Transform, the optical transfer function (OTF) are plotted in Figure 2.

The incoming light wavefront is spatially modulated such that it focuses in the vicinity of the fluorescent particles. Iterative focusing is performed with the help of a stepwise sequential iterative optimisation algorithm [21] using the directly transmitted speckle intensity as a feedback signal. Due to the optimized incoming wavefront, the intensity of the target speckle gets maximised, making it an interferometric focus of our scattering lens. Once the focus is formed, a grating like phase mask is loaded onto the SLM (as shown in Figure 1) in addition to the optimization mask, such that the focus transforms into an array of multiple foci as intended. This phase mask is computed offline using the method described elsewhere [2] and saved as a bitmap image. The underlying principle is that a scattering lens, like any lens, Fourier Transforms the incoming field in the far field. Hence when a grating is added in the incoming beam path, the interferometric focus in the far field is convolved with the diffraction orders resulting from the grating. By designing a suitable grating, the diffraction orders can be placed on a periodic grid, which upon convolution with the focus results in an array of multiple foci. This array of foci can be seen as a 2D-sinusoidally varying intensity distribution, which we call the Structured Illumination, since they are used to illuminate the underlying fluorescent beads.

The resolution enhancement obtainable with SIM depends, among other things, on the spatial period of the illuminating pattern. Diffraction limited spot spacing allows for an enhancement in resolution of a factor of two [22]. In addition, good contrast between the focal spot intensities and the background ensures a reliable extraction of high resolution information from the recorded images. We found that a good contrast periodic pattern was obtained when 9 focal spots were generated along a line, i.e a 1D array of 9 foci. Even though in principle up to 30 focal spots can
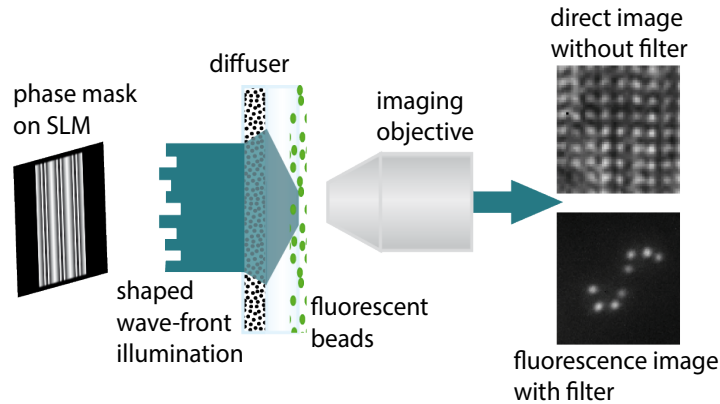
Fig. 1. Figure shows a part of the experimental setup. An illumination laser is passed through a beam expander and reflected off an SLM (illumination system not shown), showing a phase mask. The thus shaped wave-front then illuminates a by a diffuser in front of a collection of fluorescent particles. These are imaged with a detection system, including the option of introducing a fluorescence filter. A *scattering lens* produces multiple focal spots upon adding a phase mask as shown here. The mask is raster scanned to obtain a lattice of 9by9 spots. The camera sees the focal spots when no filter is added and the fluorescent beads when a filter is added.

be generated [2] [23], the corresponding low contrast illumination makes it that the captured fluorescent images also have poor contrast. Therefore there is a trade-off between the effective field of view (FOV) of the microscope, i.e the area of the illuminated region and the acquisition time of the image, which also depends on the response of fluorescence structures.

The corresponding phase mask required to generate the 9 focal spots was obtained by the methods described in [2]. In order to make a 1D array of 9 focal spots into a 2D grid, the 9 spots were raster scanned to 9 vertical positions. The CCD camera records the entire motion in one single frame, thus making up one acquisition of SIM made up of 9X9 focal spots. The vertical displacement is kept the same as the horizontal spacing, so as to make the horizontal and vertical spatial frequencies $k_x = k_y = k_0$ the same. Figure 1 shows an example of a 2D focal spot array recorded in this manner. This helps to judge the quality of illumination, which will be further used for SIM of fluorescent structures. The resulting pattern has a spatial frequency of $k_0 = 12$pixels $\approx (1.8\mu m)^{-1}$, marked by the arrow in Figure 2. The modulation contrast m of the illumination pattern is determined by the ratio $\frac{I_{max}-I_{min}}{I_{max}+I_{min}}$. For our illumination patterns, we found m to have values ranging between $0.2 - 0.4$.

3. Working of SIM

Structured Illumination Microscopy (SIM) is a super-resolution microscopy technique developed independently by Gustafsson *et al.* [24] and Heintzmann *et al.* [25]. Using SIM, a resolution enhancement of upto a factor of two over wide-field fluorescence microscopy has been demonstrated [24]. As the name suggests, the technique involves illuminating a sample with periodically varying intensity patterns i.e "Structured Illumination". The resolution enhancement aspect of SIM stems from research on OTF expansion [26] [22] and increased optical sectioning capability [27].

The technique is better understood by looking at image acquisition in frequency space rather than in image space, as the spectral content of an image neatly separates out into different frequencies. In the limit of diffraction, the maximally allowed spatial frequency is given by the OTF of the imaging system. By making use of spatially periodic illumination patterns, the
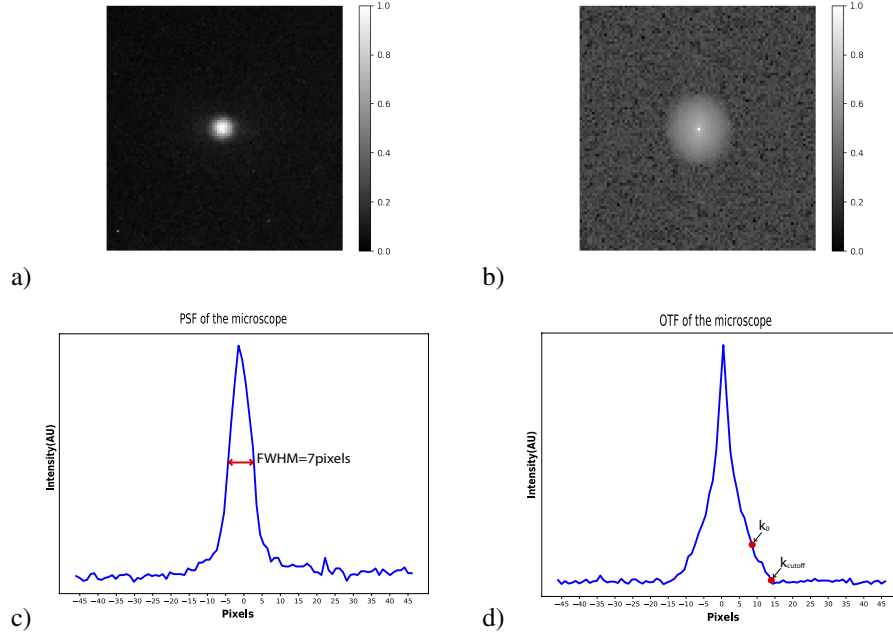
Fig. 2. a)Experimental PSF of the system measured from normalized intensity images of $0.5\mu m$ fluorescent beads. FWHM corresponds to roughly $860nm$ b) Normalized OTF of the system computed by FFT of a). c) and d) show the respective plot profiles of the PSF and OTF. The arrows mark the cutoff spatial frequency range of the detection system k_{cutoff} along with the illumination spatial frequency k_0.

sample information is coupled to the periodicity of the illumination pattern due to the Moiré effect. Thereby it down-modulates the otherwise inaccessible high frequency information to inside the reach of OTF. With a precise knowledge of the illuminating pattern, this high resolution information of the sample can be algorithmically extracted leading to an overall enhancement of resolution of the microscope. The SIM reconstruction algorithm used to process our images is adopted from an open source MATLAB toolkit called OpenSIM [28], extended further to support 2D patterned illumination.

Our multi-focal pattern can be described an intensity distribution following

$$I(x,y) = I_0[1 + m\cos(k_x x + \phi_x)][1 + m\cos(k_y y + \phi_y)] \circledast H_1(x,y) \tag{1}$$

where $k_x = k_y = k_0$ is the spatial frequency and $\phi_x = \phi_y = \phi_0$ is the phase of the illumination pattern. $H_1(x,y)$ is the PSF of the illumination objective, in our case the scattering lens. If the sample structure is represented by $S(x,y)$, the illumination with equation 1 results in a fluorescent emission with a distribution

$$D(x,y) = [S(x,y)I(x,y)] \circledast H_2(x,y) + N(x,y) \tag{2}$$

where $H_2(x,y)$ is the PSF of the imaging objective and $N(x,y)$ is the noise.

The convolution operation "$\circledast$" in equation 2 is easily dealt with upon Fourier Transformation, when it becomes a simple multiplication.

$$\widetilde{D}(k_x,k_y) = [\widetilde{S}(k_x,k_y) \circledast \widetilde{I}(k_x,k_y)]\widetilde{H}_1(k_x,k_y)\widetilde{H}_2(k_x,k_y) + \widetilde{N}(k_x,k_y) \tag{3}$$

Notice now the sample spectrum is convolved with the spectrum of the illumination pattern. For a 2D sinusoidal illumination of the form shown in Figure 3, the spectrum consists of a set of
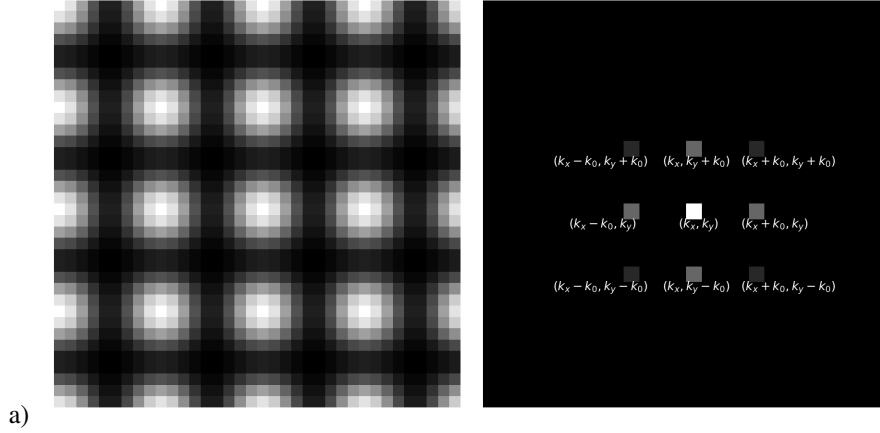
a)

Fig. 3. Simulated 2D sinusoidal illumination pattern for SIM and its corresponding frequency spectrum. The spectrum shows 9 delta peaks labelled with their corresponding spatial frequencies.

3X3 delta peaks, one at the origin and the rest located at the edge of the OTF ($\widetilde{H}_2(k_x, k_y)$) shifted in frequency by the same amount as the spatial frequency of the illumination (k_0). That is, an image acquired with such a periodic pattern is a superposition of 9 diffraction limited Fourier components given by,

$$\widetilde{D}_n(k_x, k_y) = \sum_m M_{nm} \widetilde{S}_m(k_x, k_y) \widetilde{H}_1(k_x, k_y) \widetilde{H}_2(k_x, k_y) + \widetilde{N}(k_x, k_y) \qquad (4)$$

$$\text{with} \qquad M_{nm} = \exp\left[2\pi i \left(\frac{m_x n_x}{3} + \frac{m_y n_y}{3}\right)\right]$$

where $n_x = n_y = \{0, 1, 2\}$ index the number of acquired images. Also $m_x = m_y = \{-1, 0, 1\}$ are the indices of the 3X3 set of Fourier peaks in each of the (n_x, n_y) images. In order to extract the 9 Fourier components in equation 4, we need 9 different images captured at different phase shifts of the illumination pattern. The set $D(x, y)$ in equation 2 is therefore made up of a set of in total 9 SIM images, each of which containing diffraction limited sample information. After each acquisition, the illumination pattern is shifted by an amount of $\pm 2\pi/3$ of the patterns spatial period by applying a linear gradient to the SLM. The pattern is further translated along 4 different directions capturing 3 images per direction. These phase shifted images contain the high resolution information- which we intend to extract, mixed with the diffraction limited information.

First, the noisy estimates of the sample information are obtained by inverting the mixing matrix M_{nm} and solving equation(4) for $\widetilde{S}_m(k_x, k_y)$. For a precise inversion of the equation, it is important that the matrix be non-singular.

Experimental fluctuations in the optical path or drifts of the sample may occur, which affect the precise reproducibility of the illumination pattern. Such a drift in the illumination pattern means that the phase shifts of the pattern deviate from the intended values. In the experiments, the illumination pattern generated is more or less accurately placed on a grid within a variation of about 1-2pixels, which can be enough to cause distortions in the reconstructed images. Hence there is a need to determine the phase shifts post acquisition of the SIM images.

A posteriori phase shift estimation was first introduced by K.Wicker *et al.* [29] and works by determining the matrix M_{nm}. In case of a perfect separation of Fourier components $\widetilde{S}_m(k_x, k_y)$ in equation 4, the phase shifts in the mixing matrix M_{nm} have the correct values. That is, once

the components are well separated, there is no overlapping information among the different components. With the knowledge of the phase shift matrix M_{nm}, the Fourier components $\widetilde{S}_n(k_x, k_y)$ can now be reliably extracted by

$$\text{Noisy}\left[\widetilde{S}_n(k_x, k_y)\right] = M_{nm}^{-1}\left[\widetilde{D}_n(k_x, k_y)\right] \tag{5}$$

The thus extracted off-center components are then cleaned of noise $\widetilde{N}(k_x, k_y)$ using Wiener filtering [30]. The final steps towards achieving the SIM reconstruction then consists of shifting these noise-free estimates $[\widetilde{S}_n(k_x, k_y)]_{\text{filtered}}$ of the Fourier components to their actual locations in the frequency domain and summing up over all of the components. After filtering the components, their centers are actually located at the origin of the spectrum, whereas they in fact belong at the positions k_0 away from the origin. Shifting of the components to these original locations is made possible by the Fourier Shift theorem [30]. A lateral shift of k_0 in the spatial domain is equivalent to multiplication by a phase factor $e^{-i2\pi k_0(m_x + m_y)}$ (with $m_x = m_y = \{-1, 0, 1\}$ as before). Hence, multiplication of the respective Fourier components by this phase factor will shift the corresponding real-space information by k_0. Once all the 9 components are shifted to their original locations, they are summed up. This then extends the spectrum of the image, which was conventionally limited at k_{cutoff} and is now extended to $k_{\text{cutoff}} \pm k_0$ in all directions. At this stage, the reconstructed image spectrum can be Inverse Fourier Transformed, to reveal the super-resolved image of the sample in real-space.

4. Results and Discussion

Using the procedure outlined so far, SIM images were acquired and processed to reconstruct high resolution information. The multiple focal spots that are used as illumination pattern for SIM are judged based on their intensity uniformity, spot spacing and modulation contrast. We were able to generate multiple foci with intensity uniformity close to 1, i.e almost all foci had similar intensities. The spot spacing among the foci corresponds to the spatial period of the SIM illumination. In our experiments, the spatial period was found to be $= 1.8\mu m$. Also, the modulation contrast at this spatial period was found to vary between experiments in the range of $0.2 - 0.4$.

The images of both illumination patterns and the illuminated fluorescent structures were captured, resulting in the data set $D_n(x, y)$. We first obtained the SIM images of the transmitted light without fluorescent samples in the field-of-view. After running these images through the phase determination step, we were able to obtain the experimental phase shifts. Even though the intended phase shifts were $(\pm 120, \pm 120)$ degrees, the experimentally obtained multiple foci pattern drifted from these phase shift values by about $\pm 8 - 10$ degrees. This drift in the experimental phase shift values from the intended values means that the fluorescent SIM images will also drift from the intended values by the same amount. Further when we compared phase shifts of fluorescent SIM images with the phase shifts determined from SIM images of transmitted focal spots, we saw that the phase shifts of fluorescent images deviated from that of the focal spots only by about $\pm 2 - 4$degrees. This is indeed a remarkable result of *a posteriori* phase shift determination.

The Fourier components extracted with the knowledge of their phase shifts are then Wiener filtered and shifted to their original locations. They are subsequently added together to obtain the reconstructed spectrum of the sample image. This summed up spectrum is Inverse Fourier Transformed to get the reconstruction in sample-space. With this, the reconstruction procedure is completed and a high resolution reconstruction of the image is obtained. Note however, that the cut-off of the filter introduces periodic disturbances in the inverse Fourier transform, which are visible in the reconstructions. However, these are at a different spatial frequency than the resulting resolution and are not too large in amplitude, such that the reconstructed images can still be analysed for their increase in resolution.
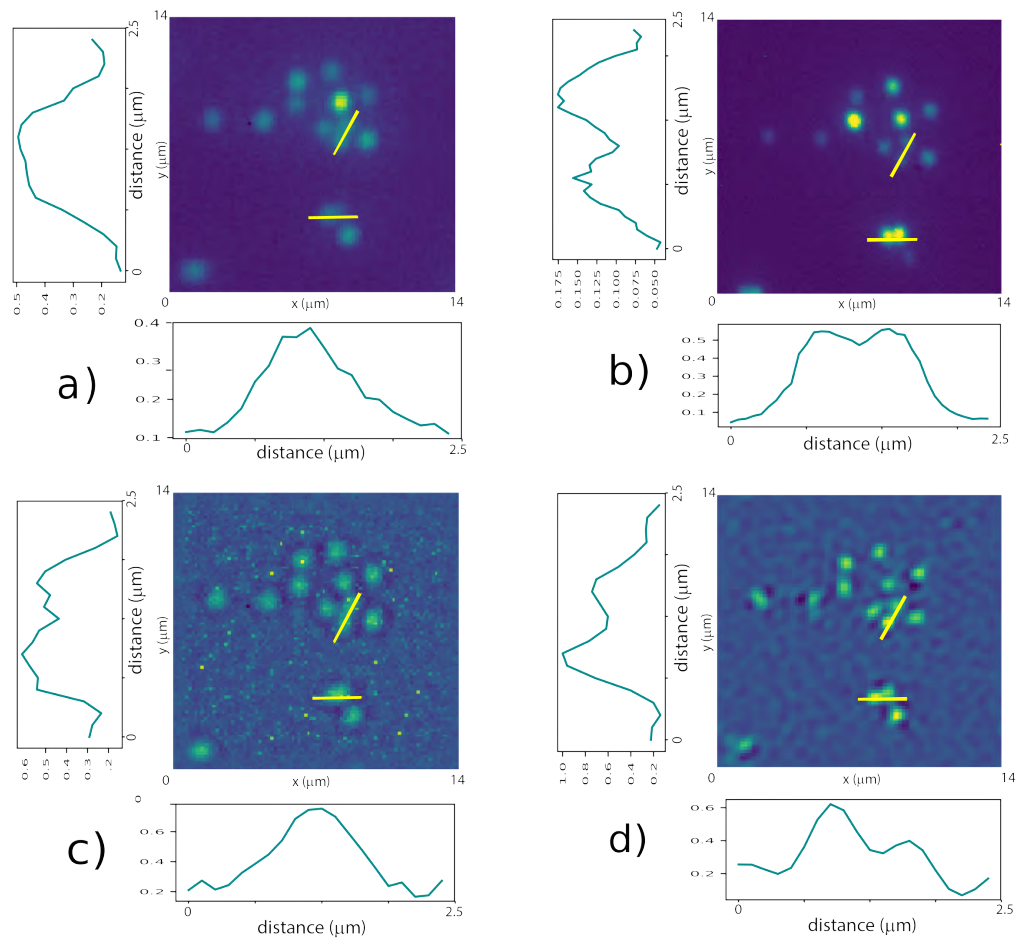
Fig. 4. SIM reconstruction: a)speckle illuminated fluorescent sample scene captured using 40X objective. b) same scene as seen with a 100X objective. c) wide-field reconstructed component taken from SIM algorithm performed with 40X objective containing only the diffraction limited information thus similar to a). d) super resolution added to the wide-field component in c). This shows a clear enhancement in resolution over c). The intensity cross-sections along the dashed yellow lines are plotted for corresponding images. Vertical plots are along the slanted lines and horizontal plots are along the horizontal lines. d) clearly shows that neighbouring beads can now be resolved. The resolution enhancement in d) is comparable to that of the wide-field image in b).

The results of our SIM reconstruction of $0.5\mu m$ sized fluorescent beads is as shown in Figure 4. As can be seen from subfigure d), the SIM reconstruction leads to enhancement in the resolution of our microscope. The intensity cross section over the beads clearly shows that using SIM, the fluorescent beads that were otherwise not resolvable are now resolved. The resolution enhancement can be compared with a widefield image obtained with another objective of superior magnification as shown in subfigure b). As the corresponding intensity cross sections show, the resolution enhancement obtained with SIM reconstruction using the 40X objective is comparable to that obtained using a 100X objective conventionally. In contrast, the wide-field component in subfigure c) cannot resolve the same features, as is the case with the direct wide-fied image at 40X resolution in subfigure a). The unresolved features in subfigure b) also demonstrate that the
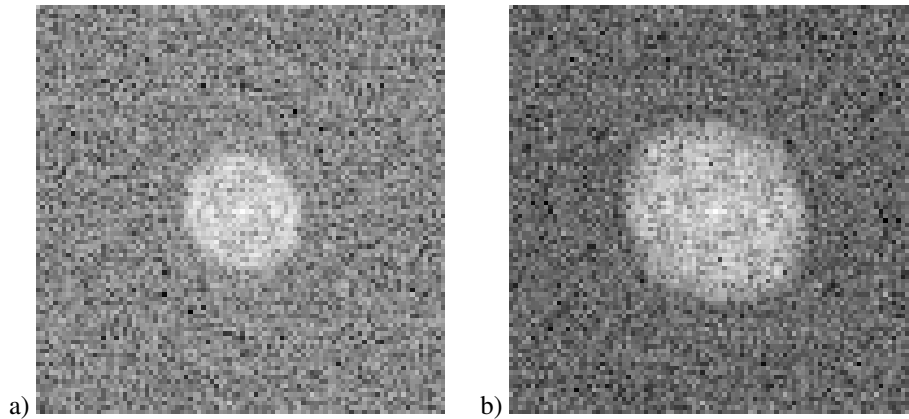
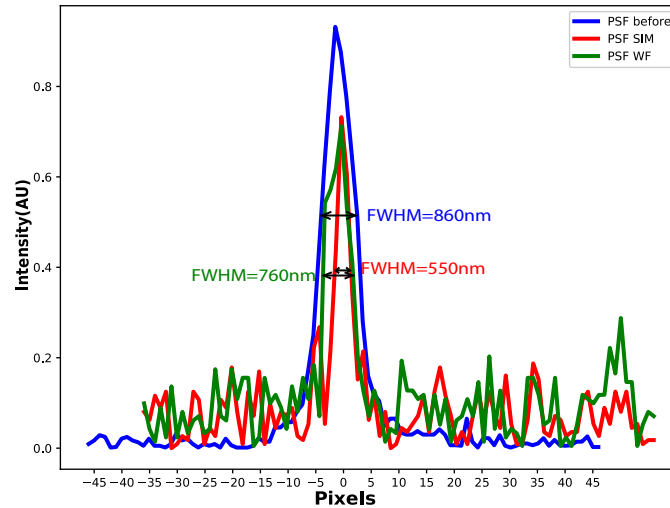Fig. 5. Widefield and SIM reconstruction spectra

Fig. 6. A plot of intensity PSF of the microscope after SIM reconstruction shows a narrowing compared to that before. For comparison the conventional widefield PSF obtained using Wiener filtering of the central unshifted component is also plotted. From these plots it is clear that the PSF is narrower due to SIM reconstruction and not due to Wiener filtering. The result corresponds to a ≈ 1.6 fold resolution enhancement.

enhanced resolution is not a result of deconvolution and filtering but rather the addition of super resolution information from the extracted high frequency components. Apart from the fact that the bead clusters are resolvable with SIM reconstruction, the figure also shows that the individual beads are much narrower in subfigure d) compared to those in a) and c). This means that the effective PSF of the microscope is narrower, which is also a sign of resolution enhancement. In frequency space, the resolution enhancement is given by the broadening of the OTF support, shown in the lateral direction of the focal plane in Figure 5, showing a clearly broadened OTF, which is roughly circular rather than petal-shaped for SIM along the optical axis.
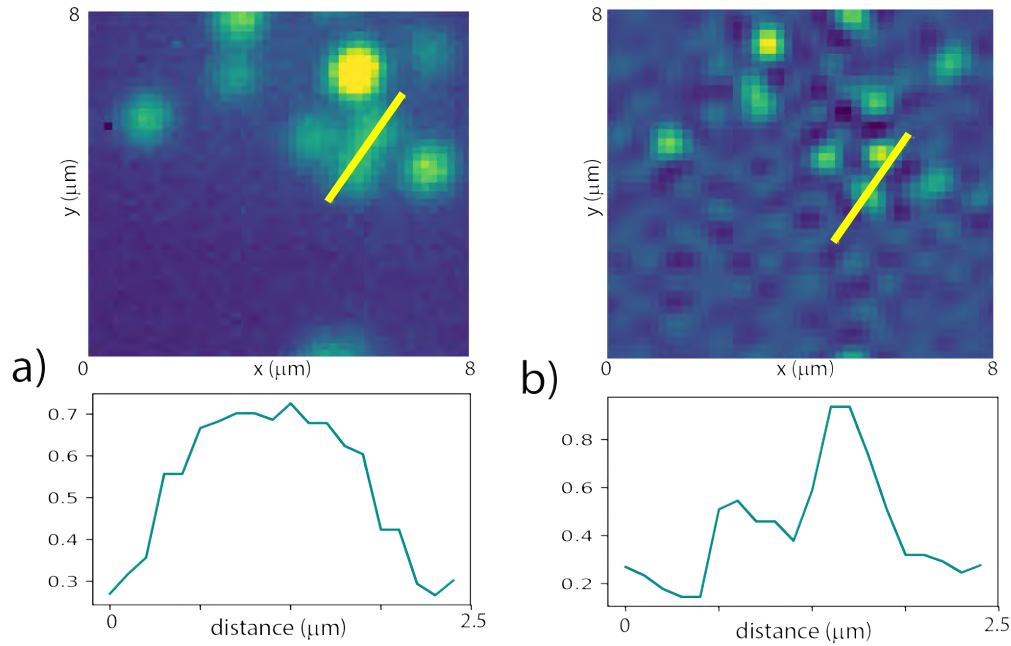
Fig. 7. SIM results with a smaller number of foci used in the periodic illumination (here a 5×5 example is shown). a)Widefield image of the scene b)SIM reconstructed image a). Their corresponding plots show that b) has superior resolution than a). SIM with reduced number of foci only implies a smaller field-of-view and does not affect resolution enhancement.

As shown in Figure 2, the spatial frequency of illumination is at ∼ 48% of the cutoff frequency of the OTF corresponding to $(1.8\mu m)^{-1}$. This implies we expect a resolution enhancement of about ∼ 48% relative to the conventional wide-field imaging. Such a resolution improvement corresponds to a narrower PSF of width of 549 nm. In order to quantify the improvement in resolution in real space, the PSF before and after SIM reconstruction are plotted in Figure 6. As shown in Figure 6, the PSF after reconstruction indeed has a FWHM of 550 nm. This means we have obtained a ≈ 1.6-fold improvement in resolution compared to the conventional wide-field microscope. The PSF of the Wiener filtered wide-field component is also plotted for comparison to show that the narrowing of PSF is due to SIM reconstruction and not simply due to deconvolution using wiener filtering. Although a full theoretical resolution enhancement of a factor two has not been achieved. This is due to the fact that we are limited by spatial frequency of SIM illumination. As the illumination frequency is not at the edge of the OTF but rather at ∼ 48% of the cutoff frequency, we are also only able to extract ∼ 48% of the super-resolution information. Nevertheless a narrower PSF due to SIM clearly shows that we are able to now access information beyond the diffraction limit of the optical system used.

The field-of-view of our scattering microscope used for SIM is currently limited by the number of foci that can be simultaneously generated. In our experiments, the area of the fluorescent samples simultaneously illuminated with a 9X9 array of foci corresponds to about ≈ $14x14\mu m^2$. This can in principle be expanded by increasing the number of foci along each direction. However, it is important to note that with the increased number of foci, their respective intensities will be effectively lower. This means that longer exposure times of the camera may have to be incorporated, which will in turn delay the total acquisition time of the SIM images. Alternatively increasing the number of foci can also achieved by simply tiling the 9 foci next to each other in each direction so as to obtain e.g. 18X18 foci thereby doubling the field of view. Another

important factor for increasing the field of view is that it greatly depends on the range of the memory effect of the scattering lens used. If the scattering lens is made up of a ground glass diffuser as is the case here, many more foci can be obtained in each direction, thereby increasing the field of view. Nevertheless, depending on the intensity of the illuminating foci and the fluorescence response from the sample, there exists a trade-off. In our experiments we could not get reasonable images with increasing the number of foci, but we did perform measurements with 5X5 foci in addition to the already described 9X9 foci. This obviously smaller field of view nevertheless did not affect the achievable resolution. But it indeed affected the total exposure time. Due to the smaller number of foci in 5X5 case, their respective intensities were much higher than in the case of 9X9 foci. So each image could be recorded much faster. Figure 7 shows the results of SIM reconstruction of a part of the scene shown in Figure 4, however illuminated with 5X5 foci, and hence a smaller field of view. As the figure shows, there is no impact on the resolution enhancement. Despite smaller area of illumination, SIM reconstruction nevertheless improves the resolution of the microscope.

5. Conclusion

We have developed a technique for super-resolution imaging behind a scattering medium. We make use of Structured Illumination Microscopy to obtain high resolution information beyond the diffraction limit of the optical system. Using wavefront shaping and interferometric light focusing through scattering media we are able to obtain a diffraction limited focus behind the medium. This focus is further split into an array of a number of foci. This way, we generate a high frequency 2D sinusoidal focal spot array behind a diffuser. We showed that a focal spot array of this sort can be used as a source of periodic illumination required to perform SIM imaging. Our results show that we are indeed able to enhance the resolution of our scattering microscope. The broadening of the system OTF after SIM reconstruction shows that we now have access to the high resolution information which was otherwise not accessible. The SIM reconstructed images of fluorescent beads are superior in resolution compared to their wide-field counterparts. A closer examination reveals about ≈ 1.6 fold improvement in resolution over conventional wide-field imaging. This is as expected from the illumination frequency used in our recorded images.

Acknowledgments

References

1. I. M. Vellekoop and C. M. Aegerter, "Scattered light fluorescence microscopy: imaging through turbid layers," Opt. Lett. **35**, 1245 (2010).
2. A. Malavalli, M. Ackermann, and C. M. Aegerter, "Structured illumination behind turbid media," Opt. Express **24**, 23018 (2016).
3. E. Abbe, "Beiträge zur theorie des mikroskops und der mikroskopischen wahrnehmung," Arch. für Mikroskopische Anat. **9**, 413–418 (1873).
4. R. C. Dunn, "Near-field scanning optical microscopy," Chem. Rev. **99**, 2891–2928 (1999).
5. S. W. Hell, "Fluorescence nanoscopy: Breaking the diffraction barrier by the RESOLFT concept," GBM Annu. Fall meeting Berlin/Potsdam 2005 **2005** (2005).
6. M. J. Rust, M. Bates, and X. Zhuang, "Sub-diffraction-limit imaging by stochastic optical reconstruction microscopy (STORM)," Nat. Methods **3**, 793–796 (2006).
7. E. Betzig, G. H. Patterson, R. Sougrat, O. W. Lindwasser, S. Olenych, J. S. Bonifacino, M. W. Davidson, J. Lippincott-Schwartz, and H. F. Hess, "Imaging intracellular fluorescent proteins at nanometer resolution," Science **313**, 1642–1645 (2006).
8. M. G. L. Gustafsson, D. A. Agard, and J. W. Sedat, "Doubling the lateral resolution of wide-field fluorescence microscopy using structured illumination," in *Three-Dimensional and Multidimensional Microscopy: Image Acquisition Processing VII,* J.-A. Conchello, C. J. Cogswell, A. G. Tescher, and T. Wilson, eds. (SPIE, 2000).

9. A. Corlu, R. Choe, T. Durduran, M. A. Rosen, M. Schweiger, S. R. Arridge, M. D. Schnall, and A. G. Yodh, "Three-dimensional in vivo fluorescence diffuse optical tomography of breast cancer in humans," Opt. Express **15**, 6696 (2007).

10. A. F. Fercher, W. Drexler, C. K. Hitzenberger, and T. Lasser, "Optical coherence tomography - principles and applications," Reports on Prog. Phys. **66**, 239–303 (2003).

11. I. M. Vellekoop, A. Lagendijk, and A. P. Mosk, "Exploiting disorder for perfect focusing," Nat. Photonics **4**, 320–322 (2010).

12. G. Ghielmetti and C. Aegerter, "Scattered light fluorescence microscopy in three dimensions," in *Biomedical Optics and 3-D Imaging,* (OSA, 2012).

13. I. Freund, M. Rosenbluh, and S. Feng, "Memory effects in propagation of optical waves through disordered media," Phys. Rev. Lett. **61**, 2328–2331 (1988).

14. G. Ghielmetti and C. M. Aegerter, "Direct imaging of fluorescent structures behind turbid layers," Opt. Express **22**, 1981 (2014).

15. S. Popoff, G. Lerosey, M. Fink, A. C. Boccara, and S. Gigan, "Image transmission through an opaque material," Nat. Commun. **1**, 1–5 (2010).

16. J. Bertolotti, E. G. van Putten, C. Blum, A. Lagendijk, W. L. Vos, and A. P. Mosk, "Non-invasive imaging through opaque scattering layers," Nature **491**, 232–234 (2012).

17. O. Katz, P. Heidmann, M. Fink, and S. Gigan, "Non-invasive single-shot imaging through scattering layers and around corners via speckle correlations," Nat. Photonics **8**, 784–790 (2014).

18. J. Schneider and C. M. Aegerter, "Guide star based deconvolution for imaging behind turbid media," J. Eur. Opt. Soc. Publ. **14** (2018).

19. E. G. van Putten, D. Akbulut, J. Bertolotti, W. L. Vos, A. Lagendijk, and A. P. Mosk, "Scattering lens resolves sub-100 nm structures with visible light," Phys. Rev. Lett. **106** (2011).

20. H. Yilmaz, E. G. van Putten, J. Bertolotti, A. Lagendijk, W. L. Vos, and A. P. Mosk, "Speckle correlation resolution enhancement of wide-field fluorescence imaging," Optica **2**, 424 (2015).

21. I. Vellekoop and A. Mosk, "Phase control algorithms for focusing light through turbid media," Opt. Commun. **281**, 3071–3080 (2008).

22. M. G. L. Gustafsson, D. A. Agard, and J. W. Sedat, "Sevenfold improvement of axial resolution in 3D wide-field microscopy using two objective lenses," in *Three-Dimensional Microscopy: Image Acquisition and Processing II,* T. Wilson and C. J. Cogswell, eds. (SPIE, 1995).

23. A. Malavalli, "Microscopy behind Turbid Media," Ph.D. thesis, Physics Institute, University of Zurich (2019).

24. M. G. L. Gustafsson, "Surpassing the lateral resolution limit by a factor of two using structured illumination microscopy. SHORT COMMUNICATION," J. Microsc. **198**, 82–87 (2000).

25. R. Heintzmann and C. G. Cremer, "Laterally modulated excitation microscopy: improvement of resolution by using a diffraction grating," in *Optical Biopsies and Microscopic Techniques III,* I. J. Bigio, H. Schneckenburger, J. Slavik, K. Svanberg, and P. M. Viallet, eds. (SPIE, 1999).

26. S. W. Hell, S. Lindek, C. Cremer, and E. H. K. Stelzer, "Confocal microscopy with an increased detection aperture: type-b 4pi confocal microscopy," Opt. Lett. **19**, 222 (1994).

27. M. A. A. Neil, R. Juškaitis, and T. Wilson, "Method of obtaining optical sectioning by using structured light in a conventional microscope," Opt. Lett. **22**, 1905 (1997).

28. A. Lal, C. Shan, and P. Xi, "Structured illumination microscopy image reconstruction algorithm," IEEE J. Sel. Top. Quantum Electron. **22**, 50–63 (2016).

29. K. Wicker, O. Mandula, G. Best, R. Fiolka, and R. Heintzmann, "Phase optimisation for structured illumination microscopy," Opt. Express **21**, 2032 (2013).

30. J. W. Goodman, *Introduction to Fourier Optics* (W.H.Freeman & Co Ltd, 2005).